Electronic Supplementary Information (ESI)

Pseudocapacitance-Boosted Ultrafast Na Storage in Pie-Like FeS@C Nanohybrid as Advanced Anode Material for Sodium-Ion Full Batteries

Bao-Hua Hou,[a] Ying-Ying Wang,[a] Jin-Zhi Guo,[a] Qiu-Li Ning,[a] Xiao-Tong Xi,[a] Wei-Lin Pang,[a] An-Min Cao,[b] Xinlong Wang[a], Jing-Ping Zhang,[a] and Xing-Long Wu[a,]*

[a] National & Local United Engineering Laboratory for Power Batteries, Faculty of Chemistry, Northeast Normal University, Changchun, Jilin 130024, P. R. China

[b] Beijing National Laboratory for Molecular Sciences (BNLMS), Key Laboratory of Molecular Nanostructure and Nanotechnology, Institute of Chemistry, Chinese Academy of Sciences (CAS), Beijing 100190, PR China.

***Corresponding Author**

E-mail address: xinglong@nenu.edu.cn

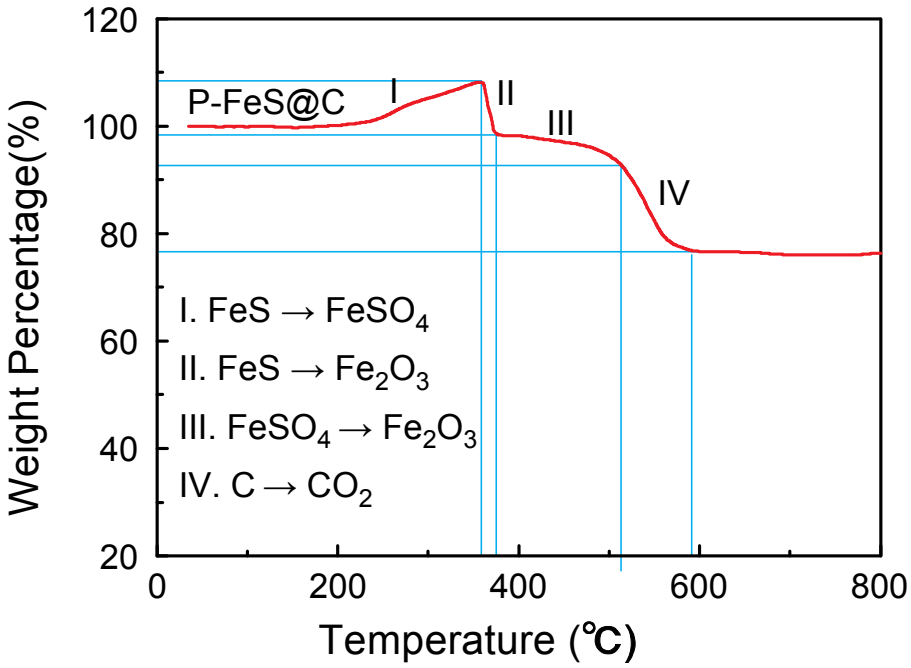

Fig. S1. TGA curve of P-FeS@C nanohybrid.

Fig. S1 reveals one-step weight gain and three-step weight loss at temperatures below 600 °C. The partial conversion reaction of FeS into $FeSO_4$ resulted in a weight increase at temperatures less than 360 °C. The steep weight loss between 360-375 °C is attributed to the decomposition of the leftover FeS into Fe_2O_3. The follow weight loss between 375-415 °C is attributed to the decomposition of $FeSO_4$ into Fe_2O_3. The final weight between loss 415-590 °C is attributed to the decomposition of C into CO_2.

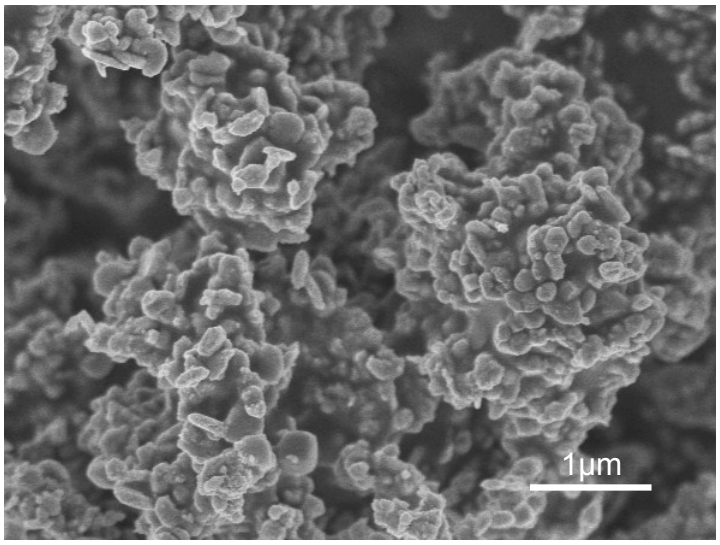

Fig. S2. SEM images of P-FeS@C nanohybrid.

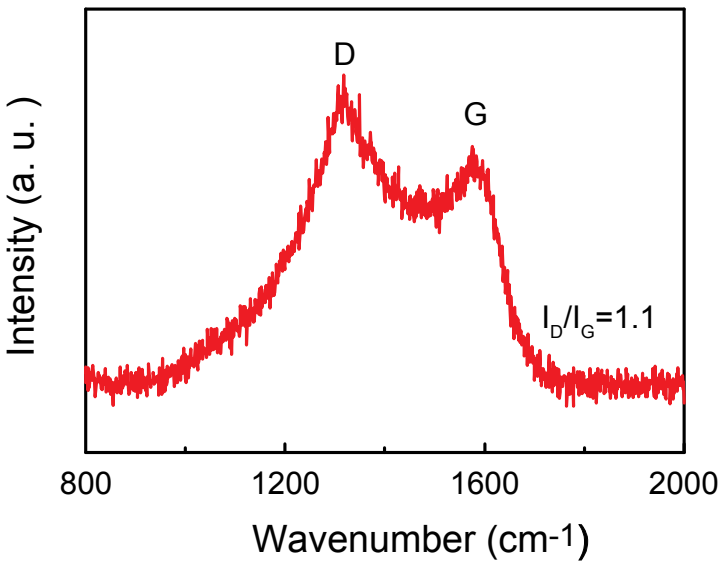

Fig. S3. Raman spectrum of P-FeS@C nanohybrid.

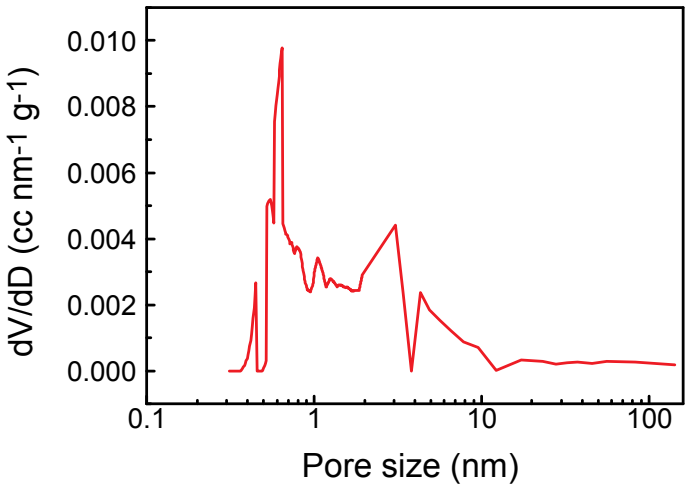

Fig. S4. The pore size distribution of the micropore + mesopores of P-FeS@C.

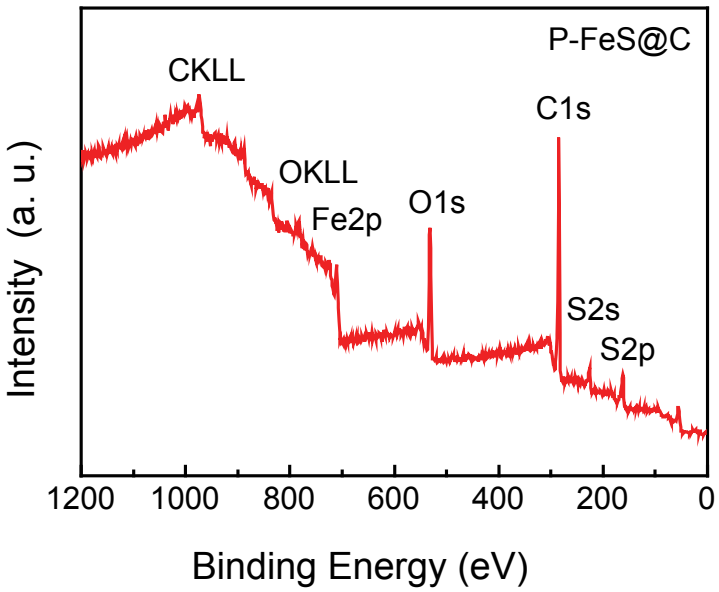

Fig. S5. XPS spectrum of P-FeS@C nanohybrid.

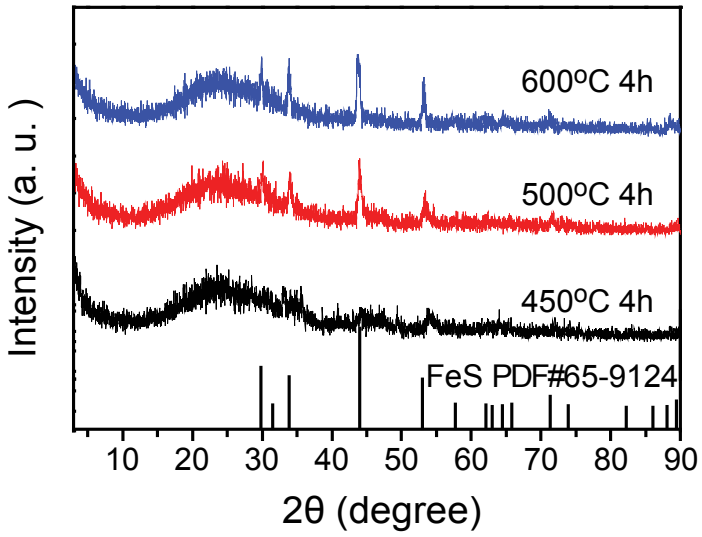

Fig. S6. XRD patterns of P-FeS@C nanohybrid prepared at different temperatures for 4h.

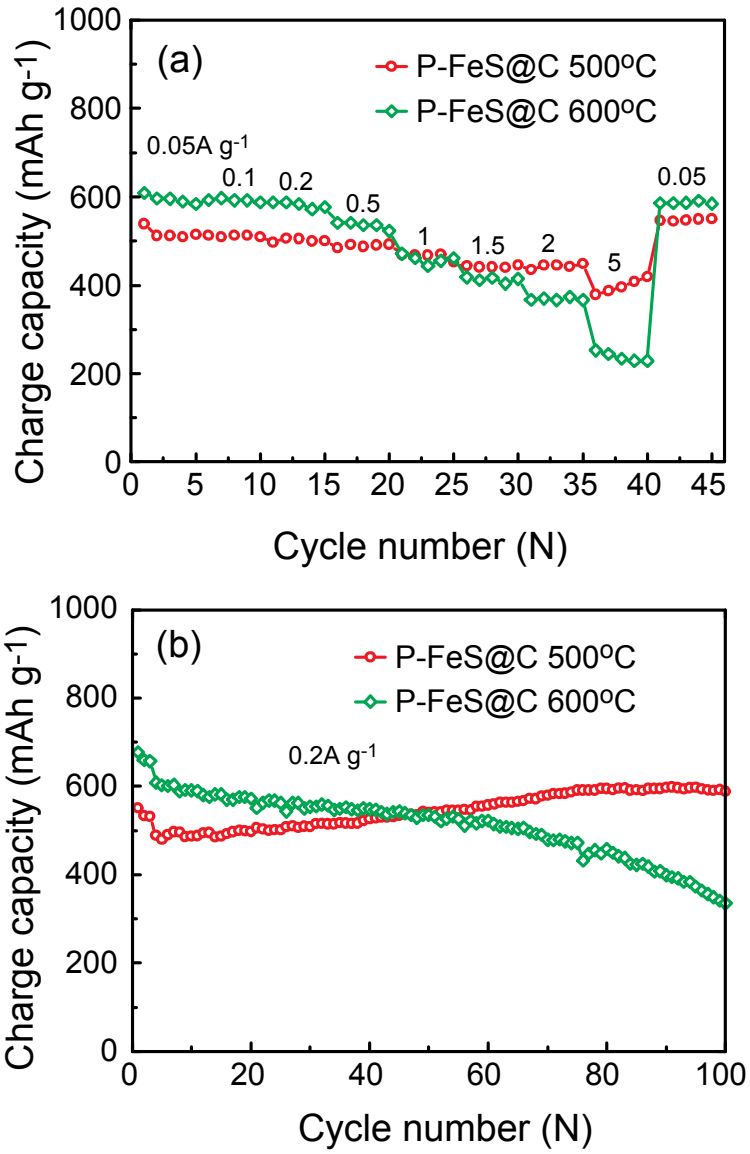

Fig. S7. The rate capability and cycling stability in the Na-ion half cells of P-FeS@C nanohybrid prepared at different temperatures for 4h.

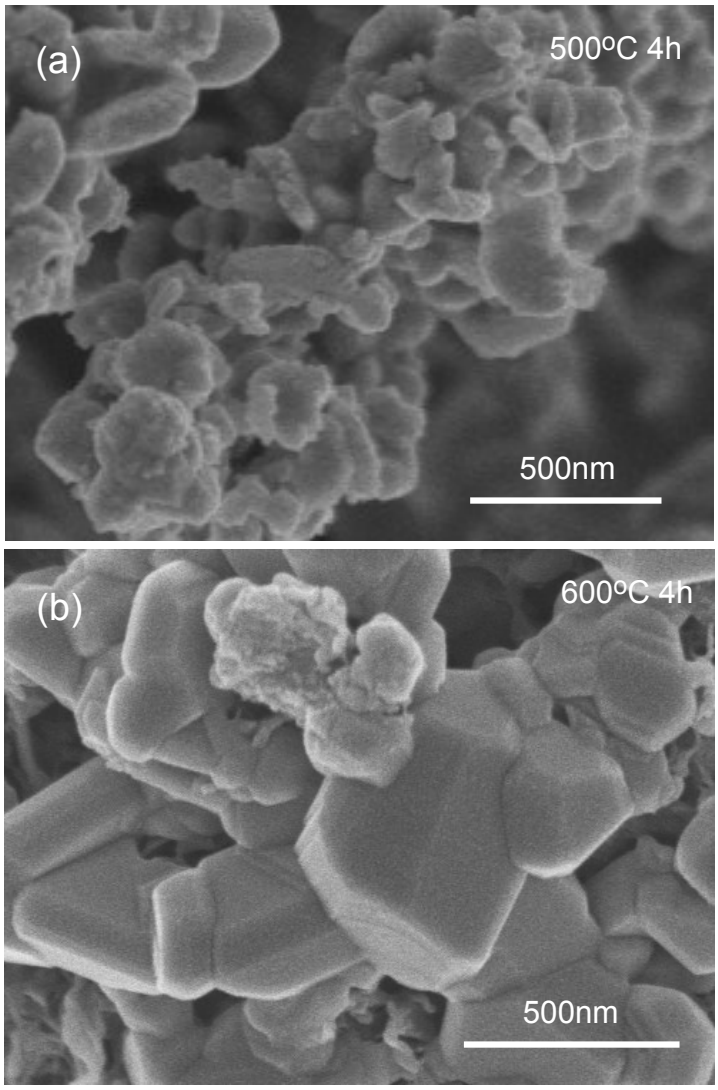

Fig. S8. The SEM images of P-FeS@C nanohybrid prepared at different temperatures for 4h.

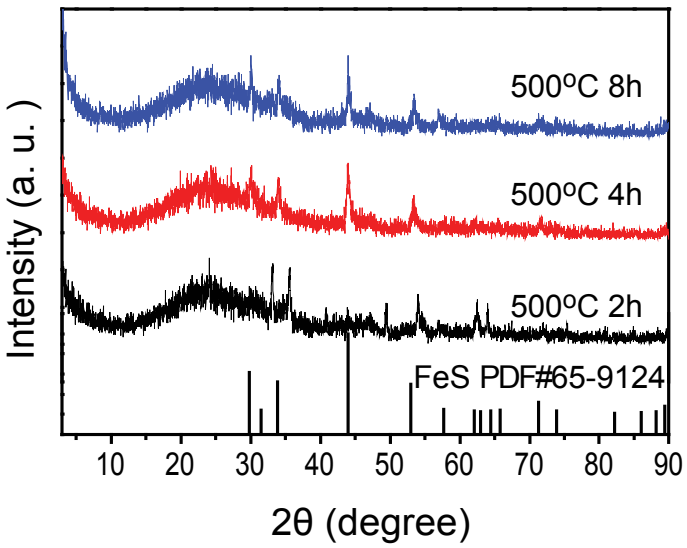

Fig. S9. XRD patterns of P-FeS@C nanohybrid prepared at 500°C for different time.

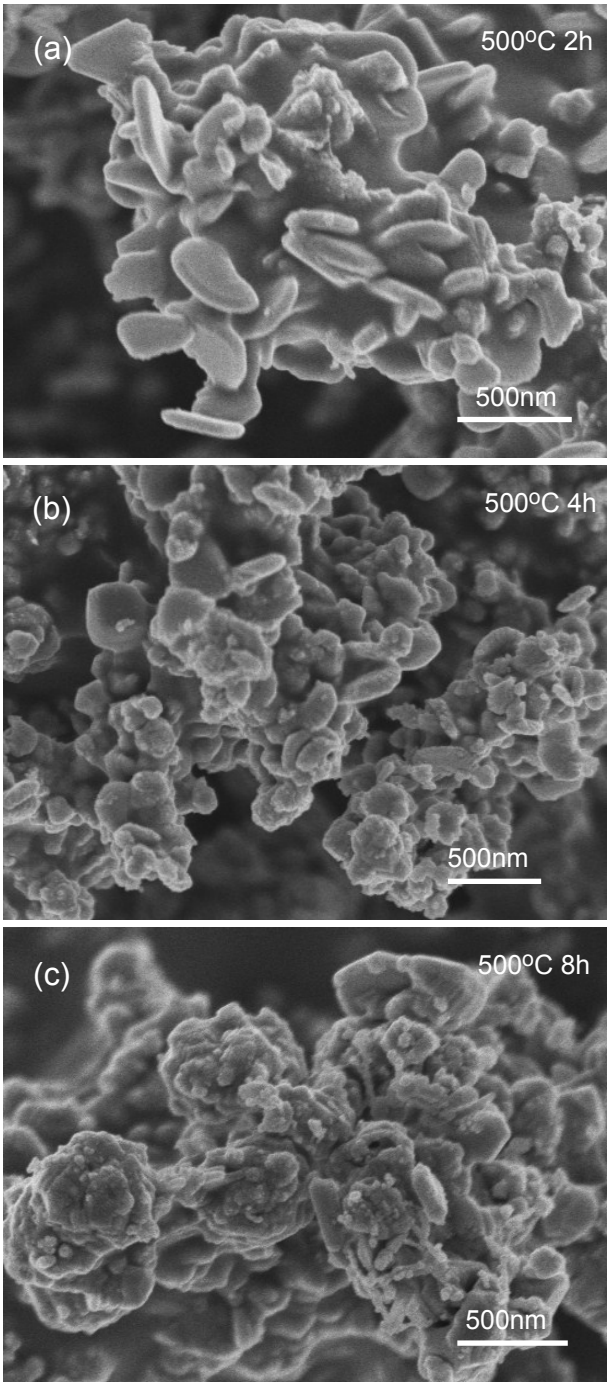

Fig. S10. The SEM images of P-FeS@C nanohybrid prepared at 500°C for different time.

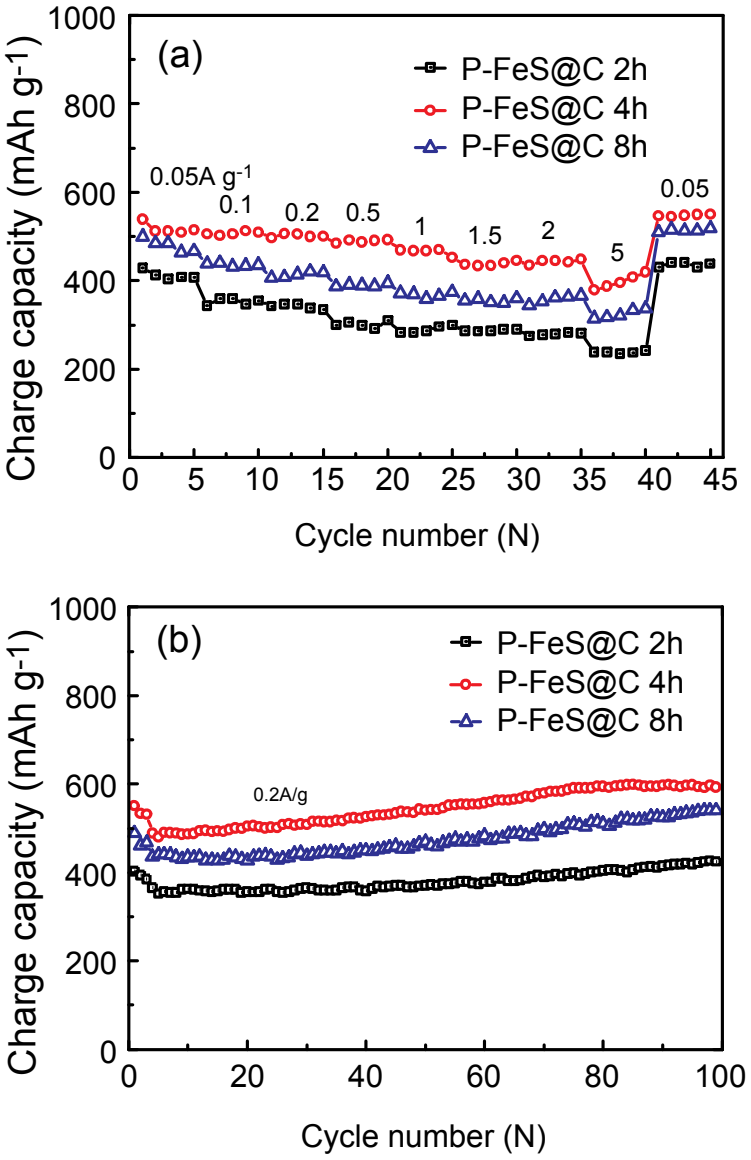

Fig. S11. The rate capability and cycling stability in the Na-ion half cells of P-FeS@C nanohybrid prepared at 500°C for different time.

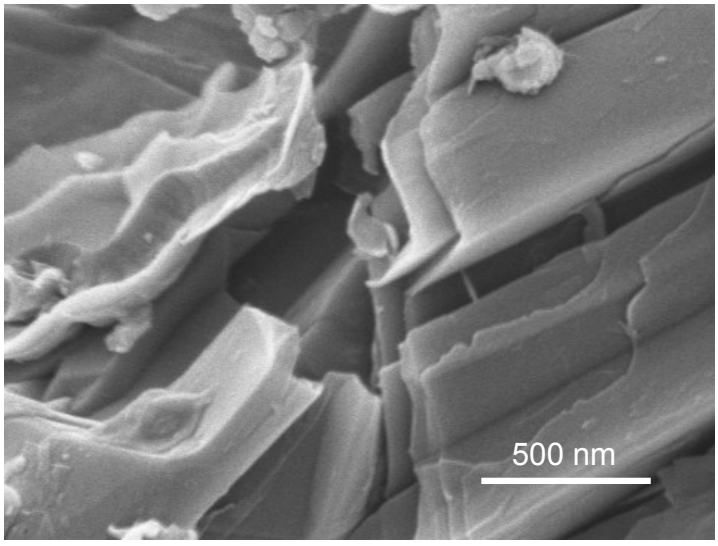

Fig. S12. SEM image of the C-FeS product.

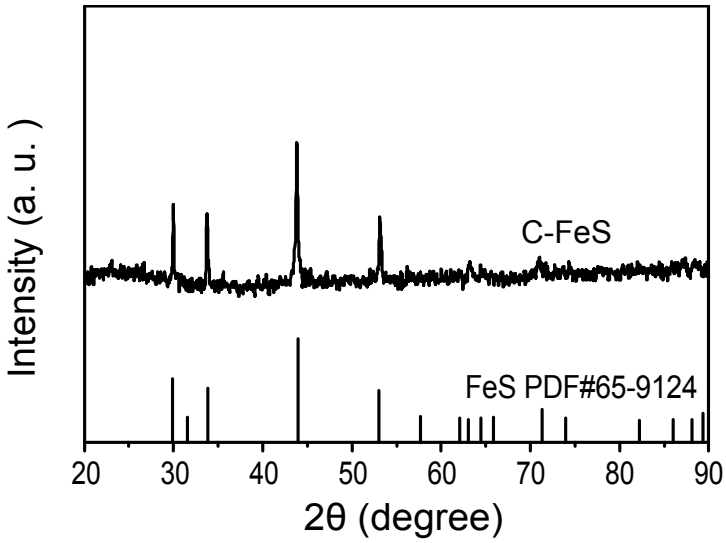

Fig. S13. XRD patterns of C-FeS.

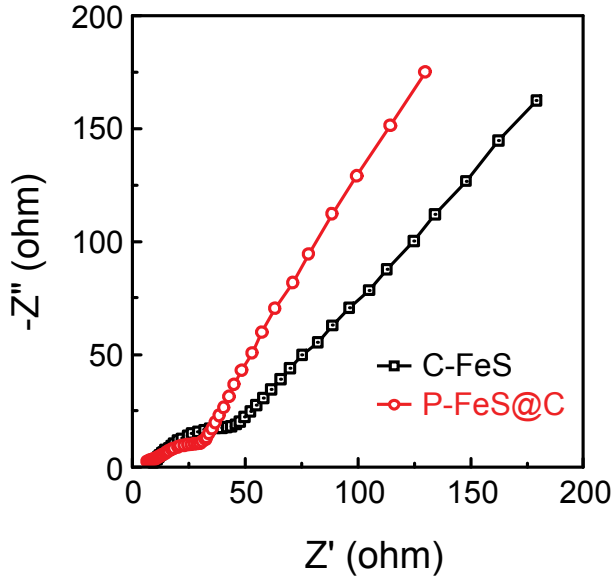

Fig. S14. Nyquist impedance plots after the first cycle of P-FeS@C nanohybrid in the Na-ion half cells.

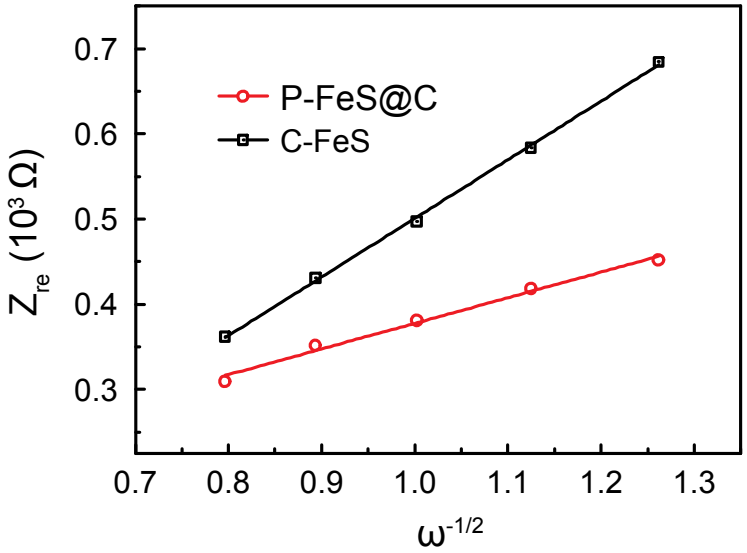

Fig. S15. The variations and fittings of Zre and $\omega^{-1/2}$ in the low-frequency region of P-FeS@C and C-FeS.

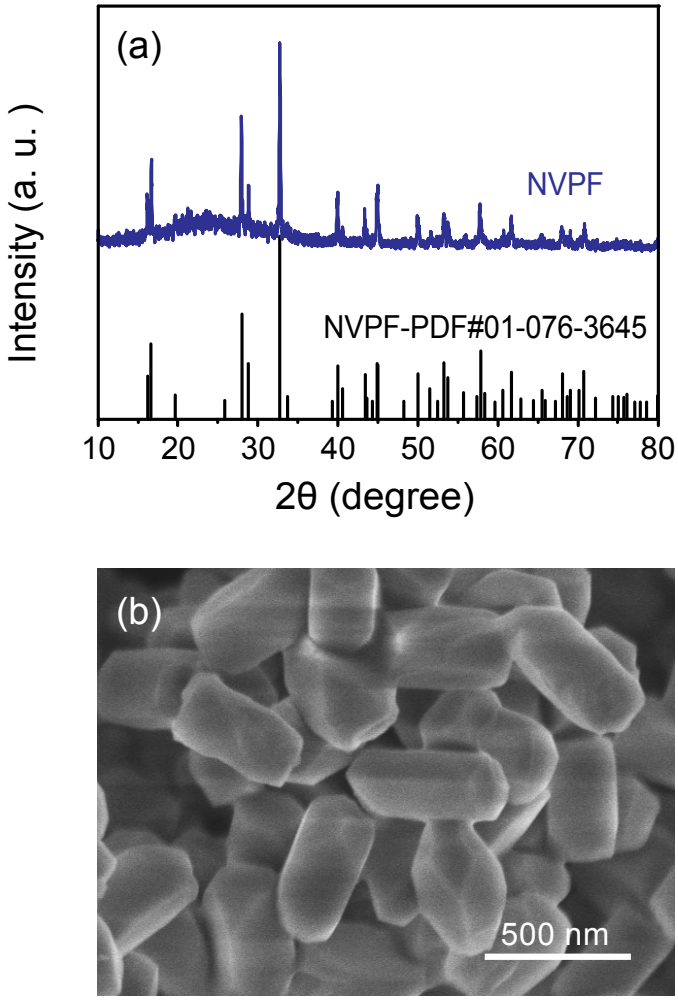

Fig. S16. (a) XRD pattern and (b) SEM image of NVPOF.

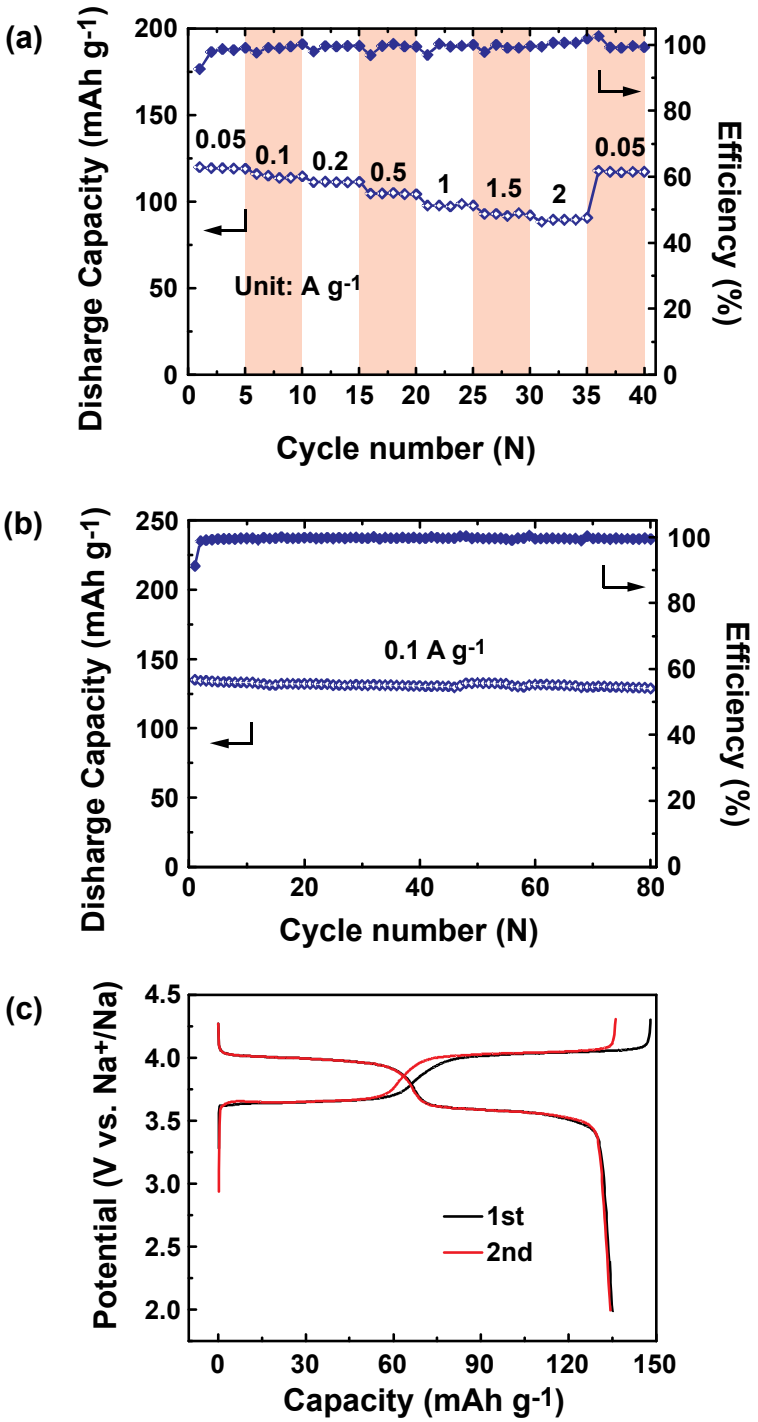

Fig. S17. (a) Rate capability, (b) Cycling stability at 0.1A g^{-1} and (c) Charge/discharge curves of NVPOF at 0.1A g^{-1} in the Na-ion half cells.